

A Study of Mechanical Advantage in Compliant Mechanisms

Gautam R. Kumar

Mechanical Engineering
Indian Institute of Science
Bangalore, 560012, India
gautam.r.kumar@gmail.com

G. K. Ananthasuresh

Mechanical Engineering
Indian Institute of Science
Bangalore, 560012, India
suresh@mecheng.iisc.ernet.in

Abstract—Understanding mechanical advantage of a compliant mechanism is not straightforward for two reasons: (i) it uses a part of the input energy in elastic deformation and (ii) its kinetoelastic behavior depends on the stiffness of the workpiece. In this paper, we study mechanical advantage using non-dimensional analysis of compliant mechanisms. We use parameterized kinetoelastostatic maps that show mechanical advantage against a non-dimensional number that captures geometric and material properties as well as forces. The maps help compare different topologies of compliant mechanisms based on mechanical advantage. The maps also help delineate kinematic and elastic contributions to mechanical advantage. Case studies reveal that while mechanical advantage usually increases with increasing external stiffness and slenderness ratio, but it decreases with increasing gap between the output port and an elastic workpiece. A noteworthy observation in this work is that there can be exceptions to this general trend and that kinematic and elastic contributions can both be positive so that the mechanical advantage of a compliant mechanism can exceed that of a rigid-body counterpart. This work also revisits the fact that it is possible to design a compliant mechanism such that its mechanical advantage is not affected by the stiffness of the workpiece.

Keywords—Compliant mechanism, mechanical advantage

I. INTRODUCTION

Compliant mechanisms transmit force, motion, and energy by virtue of elastic deformation of their constituent members. Therefore, part of the input energy that is used to deform elastic members is not available to do useful work on a workpiece or to act against an output load. The energy deficit between output and input is stored in the mechanism as elastic strain energy. Consequently, *mechanical efficiency*—defined as the percentage ratio of the output energy to the input energy—is always less than 100% for compliant mechanisms. Another consequence of inevitable strain energy in compliant mechanisms is its effect on *mechanical advantage* (MA), which is defined as the ratio of the output force to the input force.

Understanding MA of compliant mechanisms less straightforward as compared to that of rigid-body mechanisms. In rigid-body mechanisms, MA is entirely decided by kinematics. In compliant mechanisms, kinematics, forces, and elastic deformation contribute to

MA . It is worth noting that the behavior of a compliant mechanism, and hence MA too, depends on the stiffness of the workpiece.

An excellent introduction to mechanical advantage of compliant mechanisms was given by Salamon and Midha [1] in 1998. The implication of mechanical advantage in the context of design was discussed by Wang [2] in 2009. In this paper, we revisit the analysis and interpretation of mechanical advantage in compliant mechanisms to explain some new features and to present the results using non-dimensional maps that help in comparing different designs.

In Section 2, we give an introduction to mechanical advantage in compliant mechanisms by following the work of Salamon and Midha [1]. In Section 3, we consider a simple example to highlight some new features. Non-dimensional maps of mechanical advantage are presented in Section 4. Section 5 contains a discussion on the effect of workpiece stiffness on the mechanical advantage of a compliant mechanism and its implications in compliant mechanism design. Concluding remarks are in Section 6.

II. MECHANICAL ADVANTAGE OF COMPLIANT MECHANISMS

Salamon and Midha [1] defined three types of MA for compliant mechanisms. These are shown in Table 1. They differ from one another based on what quantity is fixed and what is varied among input force, output force, and output displacement. Even though some variants and combinations of these three types of mechanical advantage are conceivable, their definitions and underlying concepts seem to suffice for most practical situations.

Type 1 MA is calculated as a function of input force for a fixed value of output displacement. This definition is useful if the workpiece is assumed to be rigid. The value of output displacement would then correspond to the gap between the output point and the workpiece before the application of the input force. Thus, in elastic deformation analysis, one would need to apply the output displacement as a specified value (i.e., Dirichlet boundary condition) and compute the output reaction. Therefore, this reaction

would depend on input force as well as output displacement. This naturally leads to Type 2 *MA* wherein input force is fixed and output displacement is varied. In both types, the output reaction force is calculated and the resulting value is divided by the input force to obtain *MA*. It is possible to visualize both types of *MA* as a single surface that is parameterized using input force and output displacement.

TABLE I. TYPES OF MECHANICAL ADVANTAGE IN COMPLIANT MECHANISMS

Type	Quantity held fixed	Quantity that is varied	Quantity to be found	Definition
1	Output displacement	Input force	Output reaction force	Ratio of output reaction to input force
2	Input force	Output displacement	Output reaction force	Ratio of output reaction to input force
3	Output force (or displacement)	Stiffness of the workpiece	Input force	Ratio of output force (or reaction) to input force

Type 3 *MA* is useful where the workpiece is modeled as a spring. For simplicity, the workpiece is assumed to have linear stiffness in [1]. Whether it is linear, nonlinear, or zero, the output force and output displacement are dependent on each other. Thus, only one of them can be specified. The value of the other is then determined by the input force and the stiffness of the workpiece. As illustrated in [1], *MA* of a compliant mechanism can then be portrayed in different ways: as a function of input force for different value of stiffness, as a function output displacement (or output force) for different required values of output force (or output displacement), etc.

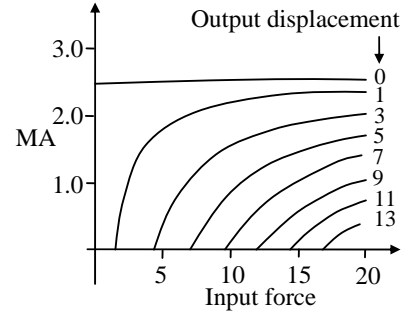
The mechanical advantage of Types 1 and 2 are shown in figs. 1(a-b) for a typical compliant mechanism [1]. Useful insight can be gained by observing the trends in *MA* of a compliant mechanism. It helps us identify useful range of input and output forces as well as output displacements at which the mechanism operates well. In most cases, *MA* is bounded above or below when a parameter is varied. This bounding value of *MA* can be interpreted as the kinematic component while the variable component can be attributed to elastic deformation. The kinematic component is essentially *MA* endowed by the inherent geometry of a given configuration of the mechanism. It may be recalled that in a rigid-body mechanism, *MA* is entirely decided by its geometry. In fact, *MA* is the reciprocal of *geometric advantage*, *GA*, which is defined as the ratio of output displacement to input displacement.

By denoting the kinematic (or rigid-body) component of *MA* as MA_r and the elastic (or compliant) component as MA_c , we write (by following [1]):

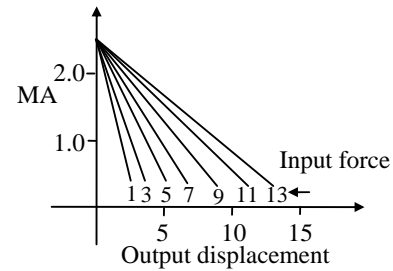
$$MA = MA_r + MA_c \quad (1)$$

This result can be analytically derived using simple work and energy arguments. Imagine that a compliant mechanism has a change in strain energy of ΔSE when it moves incrementally from a given configuration to another configuration that is very close to it. This change in strain energy is equal to the change in work done by the input and output forces, as per the principle of virtual work¹. The first order approximation of the change in work, ΔW , for a compliant mechanism with a single input and single output is

$$\Delta W = F_{in} \Delta u_{in} - F_{out} \Delta u_{out} \quad (2)$$



(a)



(b)

Fig. 1 Trends in types 1 and 2 mechanical advantage in compliant mechanisms (redrawn after [1])

where F_{in} and F_{out} are input and output forces, and Δu_{in} and Δu_{out} are the corresponding incremental displacements when the mechanism changes its configuration slightly. We can now write

$$\begin{aligned} \Delta SE = \Delta W &= F_{in} \Delta u_{in} - F_{out} \Delta u_{out} \\ \Rightarrow \frac{F_{out}}{F_{in}} &= \frac{\Delta u_{in}}{\Delta u_{out}} - \frac{\Delta SE}{F_{in} \Delta u_{out}} \Rightarrow MA = MA_r + MA_c \end{aligned} \quad (3)$$

where

$$MA = \frac{F_{out}}{F_{in}} = \text{total mechanical advantage} \quad (4)$$

$$MA_r = \frac{\Delta u_{in}}{\Delta u_{out}} = \frac{1}{GA} = \text{rigid-body component of mechanical advantage} \quad (5)$$

¹ The incremental displacement used here can be thought of as the virtual displacement, which is arbitrary as long as it is kinematically admissible. Using the Δ symbol instead of the usual δ symbol is deliberate because it makes it clear how one can use finite element analysis software to compute *MA* of compliant mechanisms.

$$MA_c = -\frac{\Delta SE}{F_{in} \Delta u_{out}} = \text{compliant component of mechanical advantage} \quad (6)$$

Equations (3) and (6) may imply that compliance (i.e., elastic deformation) decreases the mechanical advantage because MA_c is shown with a negative sign. Thus, this simple analysis highlights a seemingly inherent limitation of compliant mechanisms in that the mechanical advantage is smaller than that of an equivalent rigid-body mechanism. But one may quickly notice that MA_c can be positive if ΔSE is negative. We illustrate this in the next section with a simple pseudo rigid-body model of a compliant mechanism.

III. ANALYZING RIGID AND COMPLIANT COMPONENTS OF MECHANICAL ADVANTAGE

Consider a compliant mechanism shown in fig. 2(a) and its pseudo rigid-body model for the top-left symmetric quarter in fig. 2(b). Here, the curved beam is represented with its simplified input-output lumped model with torsional spring constants κ_1 and κ_2 at the two revolute joints of a rigid bar of length l ; sliders to account for the symmetry; and translational springs constants k_{in} and k_w to represent input-side stiffness and workpiece stiffness, respectively. The angle made by the rigid bar is denoted with θ and this angle in the initial configuration is denoted by θ_0 .

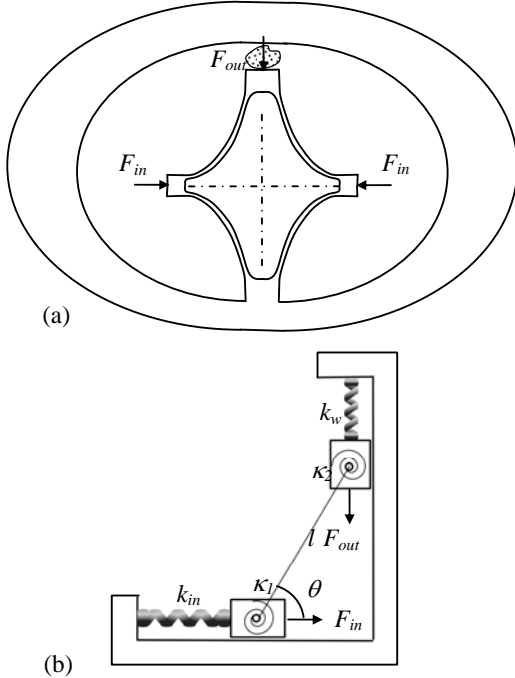


Fig. 2 (a) A compliant mechanism and (b) its lumped input-output model for the symmetric upper-right quarter.

The potential energy PE of the model in fig. 2(b) can be written as

$$PE = \frac{1}{2} k_{in} (l \cos \theta_0 - l \cos \theta)^2 + \frac{1}{2} k_w (l \sin \theta - l \sin \theta_0)^2 + \frac{1}{2} \kappa_1 (\theta - \theta_0)^2 + \frac{1}{2} \kappa_2 (\theta_0 - \theta)^2 - F_{in} (l \cos \theta_0 - l \cos \theta) + F_{out} (l \sin \theta - l \sin \theta_0) \quad (7)$$

The force equilibrium equation can be obtained by differentiating PE with respect to θ , which is a configuration variable of this single degree-of-freedom system, and equating it to zero.

$$\begin{aligned} \frac{d(PE)}{d\theta} &= 0 \\ \Rightarrow k_{in} l^2 (\cos \theta_0 - \cos \theta) \sin \theta + k_w l^2 (\sin \theta - \sin \theta_0) \cos \theta \\ &+ \kappa_1 (\theta - \theta_0) - \kappa_2 (\theta_0 - \theta) - F_{in} l \sin \theta + F_{out} l \cos \theta = 0 \end{aligned} \quad (8)$$

Upon re-arranging the preceding equation, we can write the expression for MA and split it into its rigid and compliant parts:

$$\begin{aligned} \frac{F_{out}}{F_{in}} = MA &= \frac{-k_{in} l (\cos \theta_0 - \cos \theta) \sin \theta - k_w l (\sin \theta - \sin \theta_0) \cos \theta}{F_{in} \cos \theta} \\ &- \frac{(\kappa_1 - \kappa_2)(\theta - \theta_0)}{F_{in} l \cos \theta} + \tan \theta \\ \Rightarrow MA &= \{ \tan \theta \} - \\ &\left\{ \frac{k_{in} l^2 (\cos \theta_0 - \cos \theta) \sin \theta + k_w l^2 (\sin \theta - \sin \theta_0) \cos \theta + (\kappa_1 + \kappa_2)(\theta - \theta_0)}{F_{in} l \cos \theta} \right\} \\ MA &= MA_r + MA_c \end{aligned} \quad (9)$$

By noting that $u_{out} = l (\sin \theta - \sin \theta_0)$, we can cast (9) as follows so that the expression for MA follows the format given in (3)

$$MA = [\tan \theta] - \left[\frac{k_{in} l^2 (\cos \theta_0 - \cos \theta) (\sin \theta - \sin \theta_0) \tan \theta}{\{F_{in}\} \{l (\sin \theta - \sin \theta_0)\}} \right] - \left[\frac{k_w l^2 (\sin \theta - \sin \theta_0)^2 + (\sin \theta - \sin \theta_0) (\kappa_1 - \kappa_2) (\theta - \theta_0)}{\{F_{in}\} \{l (\sin \theta - \sin \theta_0)\} \cos \theta} \right]$$

For a small increment of angle $\Delta \theta$ from θ_0 , i.e., for $\theta = \theta_0 + \Delta \theta$, we can approximate two terms in Eq. (10) as follows.

$$\begin{aligned} \cos \theta - \cos \theta_0 &= -\Delta \theta \sin \theta_0; \quad \text{and} \\ \sin \theta - \sin \theta_0 &= \Delta \theta \cos \theta_0 \end{aligned} \quad (11)$$

By using (11) and $u_{out} = l (\sin \theta - \sin \theta_0)$, Eq. (10) can be re-written as

$$MA = [\tan \theta] - \left[\frac{\left\{ \begin{array}{l} -k_{in} l^2 \sin \theta_0 \cos \theta_0 \tan \theta + \\ k_w l^2 \cos^2 \theta_0 + \frac{\cos \theta_0 (\kappa_1 - \kappa_2)}{\cos \theta} \end{array} \right\} (\Delta\theta)^2}{F_{in} \Delta u_{out}} \right] \quad (12)$$

It can be seen that it is consistent with (3) because MA_r is equal to $\tan \theta$ in this problem, as may be verified from fig. 2(b) without including the springs. Thus, by comparing (3) and (12), we have

$$\Delta SE = \left\{ \begin{array}{l} -k_{in} l^2 \sin \theta_0 \cos \theta_0 \tan \theta + k_w l^2 \cos^2 \theta_0 \\ + \frac{\cos \theta_0 (\kappa_1 - \kappa_2)}{\cos \theta} \end{array} \right\} (\Delta\theta)^2 \quad (13)$$

and therefore, as in Eq. (6),

$$MA_c = -\frac{\Delta SE}{F_{in} \Delta u_{out}} \quad (14)$$

Now, it can be seen that whenever ΔSE in Eq. (13) becomes negative, we have positive contribution from MA_c . This analysis illustrates that the mechanical advantage of a compliant mechanism can be more than that of its rigid-body counterpart. We consider some numerical data to show this.

Type 3 MA of the model in fig. 2(b) is shown in fig. 3. The plot was created for a sample data set shown in Table 2. Figure 3 shows that MA_c is positive throughout the range of F_{in} . Thus, this simple example illustrates that the mechanical advantage of a compliant mechanism can be larger than that of its rigid-body counterpart. As noted earlier, ΔSE needs to be negative for this to happen. The negativity of ΔSE requires that the instantaneous stiffness of the compliant mechanism be negative. Indeed, it is so in this case. Negative stiffness may cause instability during the operation of the device but the combination with workpiece of positive stiffness may compensate for this.

As a consequence of the instantaneous negative stiffness, another significant difference from the mechanical advantage plots given by Salamon and Midha [1] can be observed here. For the same numerical data of Table 2, we plot the mechanical advantage as a function of input force for different values of workpiece stiffness in fig. 4. Here, it can be seen that the mechanical advantage decreases with increasing workpiece stiffness.

Thus, through a simple example, we showed that the mechanical advantage of a compliant mechanism can be tailored to obtain desired trends. Next, we consider non-

dimensional plots to show trends in mechanical advantage of general compliant mechanisms.

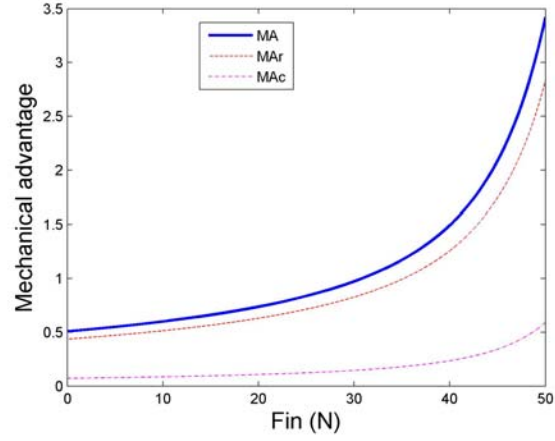


Fig. 3 Mechanical advantage and its rigid and compliant parts for the model shown in fig. 2(b)

TABLE II NUMERICAL DATA FOR THE PLOTS SHOWN IN FIG. 3

Quantity	Numerical value
l	0.25 m
k_{in}	0 N/m
k_w	100 N/m
κ_1	5 N.m/rad
κ_2	8 N.m/rad
θ_0	23.58°

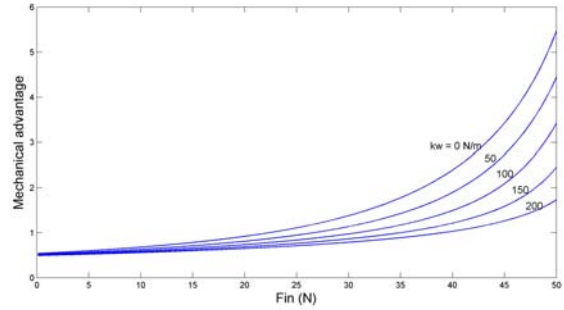


Fig. 4 Mechanical advantage as a function input force for varying workpiece stiffness for the model in Fig. 2(b) and numerical data in Table II

IV. NON-DIMENSIONAL PORTRAYAL OF MECHANICAL ADVANTAGE

A simplified lumped model was used in the preceding section to put forth some observations. Doing the same with a typical compliant mechanism may become unwieldy because it will contain too many parameters to articulate insights such as the ones described in Sections 2 and 3. Therefore, we use non-dimensional maps in this section.

Figure 5 shows non-dimensionalized transverse displacement u_{mid} of the midpoint of a fixed-fixed beam

of length L under transverse force F at the midpoint. Here, u_{mid}/L is shown against a non-dimensional number η , which captures force, geometry, and material properties as follows.

$$\eta = \frac{Fs^2}{Ebd} \quad (15)$$

$$s = \frac{\bar{l}}{d} \quad (16)$$

E is Young's modulus, b and d are the breadth and depth of the rectangular cross-section of the beam so that the area moment of inertia is given by $bd^3/12$. As discussed in [3], the kinetoelastostatic map shown in fig. 5 captures the complete nonlinear elastostatic behavior of the fixed-fixed beam under a concentrated load at its midpoint when only the displacement of the midpoint is of interest. That is, for any values of F , E , L , d , and b , we can quickly obtain u_{mid} . It is worth noting the limits of non-dimensional displacement from the figure and the role the slenderness ratio plays. In fact, the slenderness ratio s parameterizes the map in fig. 5. Details can be found in [3, 4].

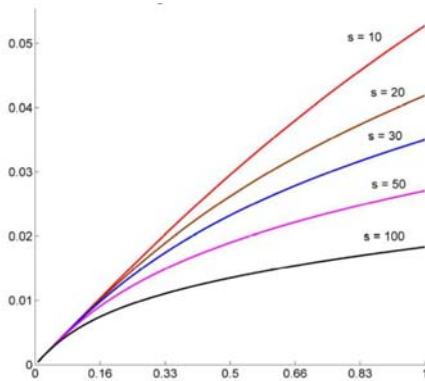


Fig. 5 Non-dimensional displacement of the midpoint of a fixed-fixed beam shown against a non-dimensional number, η .

The non-dimensional maps of the kind shown in fig. 5 can be drawn for any compliant mechanism whose geometric proportions are fixed at two levels. At one level, the lengths of beam segments should retain their relative proportions. At another level, independent of the first level, proportions of the cross-sectional dimensions of the beam segments should also retain their relative proportions. Under these conditions, the maps can be drawn for any compliant mechanism comprising multiple beam segments. In those cases, η is defined using average values of the geometric parameters of all the beam segments. Similarly, if there are multiple forces, the proportions of the magnitudes of forces should be held constant and the average value of the forces is to be used in η . The same applies to E if the beams segments are made of different materials.

As the mechanical advantage is also a non-dimensional number, it can be readily plotted against η . For the compliant mechanism in fig. 6(a) with its dimensions indicated in fig. 6(b), the non-dimensional map of mechanical advantage is shown in fig. 7. The data for this plot and all that follow from here onwards was obtained by performing multiple runs of finite element analysis using Abaqus [5]. For creating fig. 7, the non-dimensional gap (gap divided by L) is 0.0058, slenderness ratio of 170, and workpiece stiffness of 5 N/m were used. Here, gap denotes the space between the output point and the workpiece when the input force is zero. This gap must be closed first by applying some input force before mechanical advantage can be defined. The non-dimensional gap obtained by dividing by the average length is shown in fig. 7. The workpiece stiffness is not non-dimensionalized because it is independent of the mechanism and different applications may have different absolute values of workpiece stiffness.

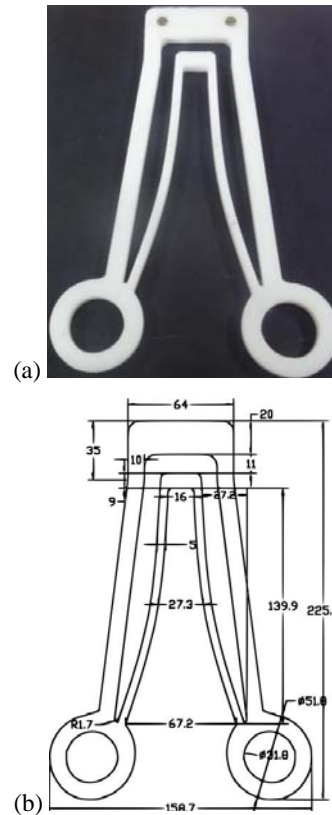


Fig. 6 (a) A compliant crimping mechanism, and (b) its dimensions in mm

Much insight can be gleaned from fig. 7. It shows that no matter what the overall size of the mechanism is, whatever its cross-section dimensions, material, and applied force are, it cannot have mechanical advantage exceeding 4 when $s = 170$, $g/L = 0.0058$, and $k_w = 5$ N/m. Thus, the limits of the mechanical advantage of a given compliant mechanism (of course, with fixed proportions as noted earlier) can be understood from a single non-

dimensional plot. Furthermore, we can also see that maximum MA is possible at $\eta \approx 10$. This means that, when mechanical advantage is the main criterion, then the geometry, material, and forces of a compliant mechanism should be chosen so that the value of η is about 10. Even when some of the parameters listed in the preceding sentence are not at the discretion of the designer, the values of the others can be chosen to accommodate the required value of η .

Figures 8(a-c) show the trends in mechanical advantage for different values of the gap, slenderness

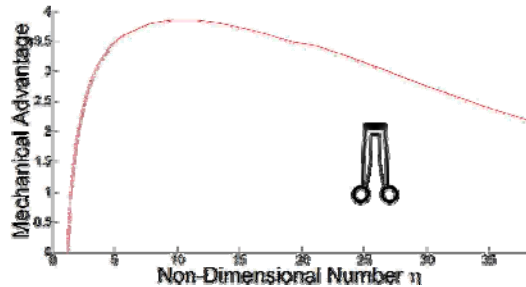
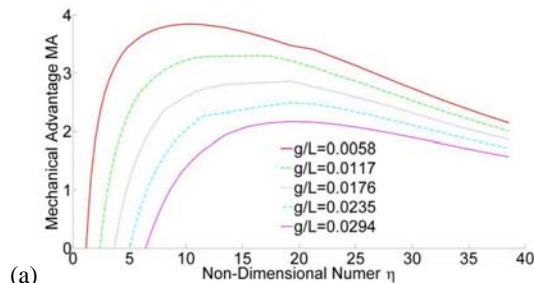
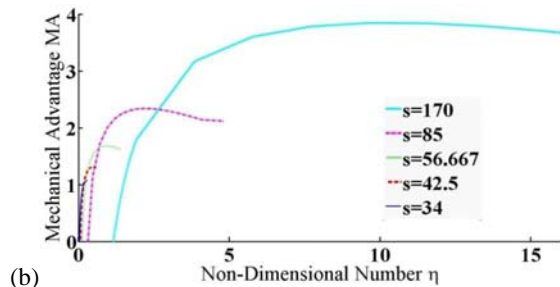


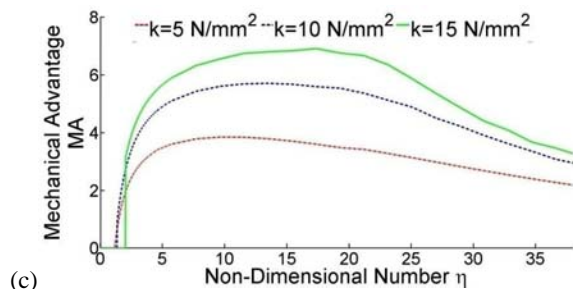
Fig. 7 Mechanical advantage vs. non-dimensional parameter of the mechanism in fig. 6(a)



(a)



(b)



(c)

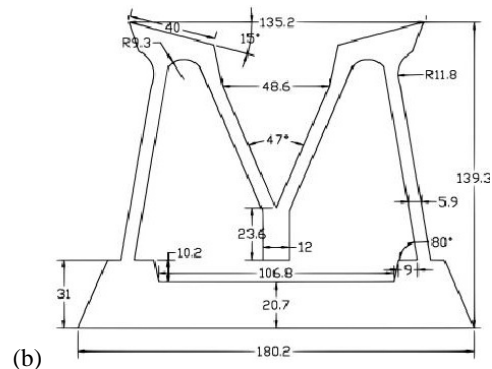
Fig. 8 Mechanical advantage for (a) different non-dimensional gaps, (b) different slenderness ratios, and (c) different values of workpiece stiffness, for the compliant crimper of Fig. (6b)

ratio, and workpiece stiffness. It can be observed from Fig. 8(a) that the mechanical advantage decreases with increasing gap. This makes sense because much larger input force is needed to close larger gaps. Figure 8(b) shows that mechanical advantage increases with increasing slenderness ratio. This means that the more flexible the mechanism is the more the mechanical advantage because large slenderness ratio implies enhanced flexibility. Furthermore, from fig. 8(c), we can see that mechanical advantage increases with increasing workpiece stiffness. It may be recalled from Section 3 that this may not always be the case.

As another example, consider the compliant mechanism in fig. 9(a) with its dimensions noted in fig. 9(b). Figures 10(a-d) illustrate trends in mechanical advantage of this mechanism; (a) with zero gap, (b) with different gaps, (c) with zero gap but different slenderness ratios, and (d) with zero gap and different workpiece stiffnesses.



(a)



(b)

Fig. 9 (a) A compliant mechanism and (b) its dimensions

One more use of the non-dimensional portrayal of mechanical advantage is that they help in comparing different compliant mechanisms. For instance, even though the functionality of mechanisms in figs. 6(a) and 9(a) is the same, the upper limit of mechanical advantage in the first mechanism is twice as much as that of the second. It can also be observed that the mechanical advantage of the second mechanism is not affected by the workpiece stiffness as much as it does in the first mechanism. This leads us to study the sensitivity of a compliant mechanism to the stiffness of the workpiece.

V. SENSITIVITY TO STIFFNESS OF THE WORKPIECE

Sensitivity index is another significant parameter in designing compliant mechanisms. Salamon and Midha [1] defined sensitivity index as the sensitivity of mechanism performance to the stiffness of the workpiece. By minimizing the energy stored in the mechanism during deformation, we can reduce the dependence of the mechanism on the stiffness of external workpiece. The general relation between sensitivity index and MA is as follows:

$$MA = MA_s \left(\frac{k}{s_k + k} \right) \quad (17)$$

where k is the stiffness of the external workpiece and MA_s is the bounding value of the mechanical advantage

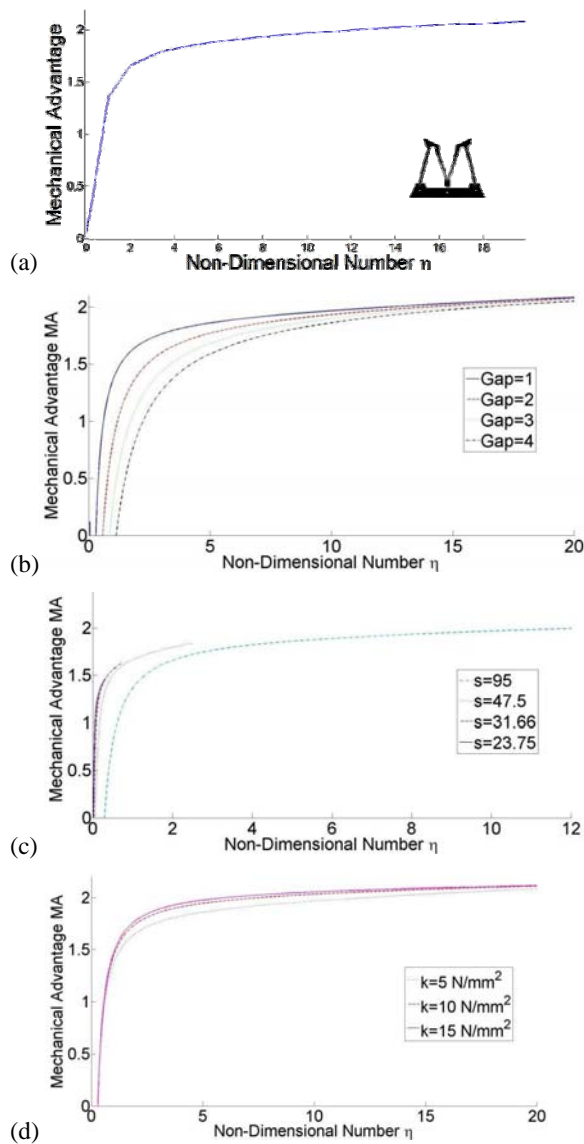


Fig. 10 The trends in mechanical advantage of the compliant mechanism of fig. 9(a).

vs. workpiece stiffness curve, shown in figs. 11 and 12 for constant force for compliant mechanisms in figs. 6a and 9a, respectively.

By fitting a curve based on (17) to the plot in fig. 11, the value of sensitivity index is found to be 0.48. This means that the effect of the stiffness of the external workpiece on the total mechanical advantage of the mechanism is small. This can be verified by observing fig. 10(d). The graph is plotted for three different values of external workpiece stiffness and we see that mechanical advantage is almost the same for all the three cases. Thus we can conclude that stiffness of the external workpiece has very little effect on the mechanical advantage of that mechanism due to sensitivity index being small in comparison to the value of k .

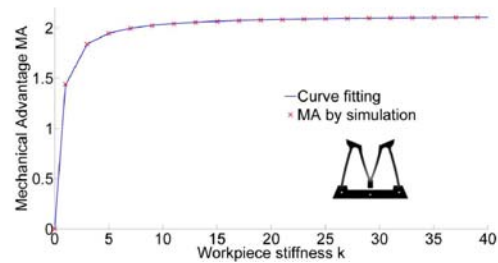


Fig. 11 Mechanical advantage vs. workpiece stiffness of the mechanism shown in fig. 9a.

Figure 12 shows the mechanical advantage vs. workpiece stiffness variation for a constant input force of mechanism in fig. 6a. The value of sensitivity index obtained through curve-fitting for this mechanism equal to 5.12. This means that the external workpiece stiffness has significant effect on the total mechanical advantage. Observing fig. 8(c), we can notice a noteworthy change of mechanical advantage with change in external stiffness and thus corroborating the higher value of sensitivity index for the mechanism in fig. 6a.

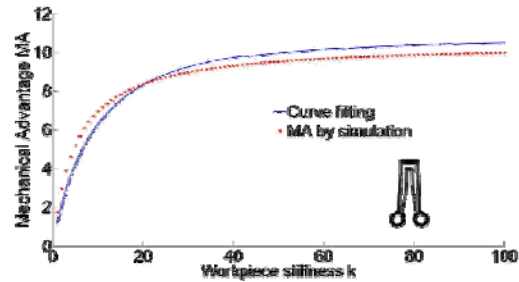


Fig. 12 Mechanical advantage vs. workpiece stiffness of the mechanism shown in fig. 6a.

VI. CONCLUSIONS

In this paper, we revisited the issue of mechanical advantage in compliant mechanisms following the work of Salamon and Midha [1]. We show two additional features that can exist in compliant mechanisms: (i) compliant component of the mechanical advantage can be

positive and thus making the mechanical advantage of a compliant mechanism larger than that of its rigid-body counterpart, and (ii) a compliant mechanism may be designed so that its mechanical advantage decreases, increases, or remains the same with respect to a large range of workpiece stiffness. We also presented non-dimensional portrayal of mechanical advantage so that much insight can be gained about the mechanism. Furthermore, different compliant mechanisms can be easily compared using the non-dimensional plots. Future work will focus on using the sensitivity index to design compliant mechanisms that not only have large mechanical advantage but are also insensitive to workpiece stiffness. Thus, we can make compliant mechanisms as attractive as rigid-body linkages from the viewpoint of mechanical advantage.

REFERENCES

- [1] B. A. Salamon, and A. Midha, "An introduction to mechanical advantage in compliant mechanisms," *Journal of Mechanical Design*, Transactions of the ASME, 120 (1998), pp. 1-5.
- [2] M. Y. Wang, 2009, "Mechanical and Geometric Advantages in Compliant Mechanism Optimization," *Frontiers of Mechanical Engineering in China*, Vol.4(3), pp. 229–241, 2009.
- [3] Harish I. Varma, Santosh D. B. Bhargav, G. K. Ananthasuresh, "Non-dimensional Kinetoelastostatic Maps for Compliant Mechanisms," ASME IDETC/CIE 2013, paper no. DETC2013-12178, held at Portland, OR, USA, Aug. 4-7, 2013.
- [4] Harish I. Varma, *Feasible and Intrinsic Kinetoelastostatic Maps for Compliant Mechanism*, MSc Thesis, Mechanical Engineering, Indian Institute of Science, Bangalore, 2013.
- [5] User manual of Abaqus finite element software, www.simulia.com.